Operational coefficient of consolidation around a pile group driven in clay/silt

Operational coefficient of consolidation around a pile group driven in clay/silt

Bryan A. McCabe[1]*, Brian G. Sexton[1] and Barry M. Lehane[2]

[1]College of Engineering and Informatics, National University of Ireland, Galway, Ireland
[2]Department of Civil and Resource Engineering, University of Western Australia, Perth, Australia

*Corresponding author. Phone: +353 91 492021, Fax: +353 91 494507, Email: bryan.mccabe@nuigalway.ie

Word Count: 4119

Keywords: pile group, pore pressure dissipation, coefficient of consolidation, uncoupled consolidation theory

Reference: McCabe, B.A., Sexton, B.G. and Lehane, B.M. (2013) Operational coefficient of consolidation around a pile group in clay-silt, *Geotechnical and Geological Engineering*, (Springer), Issue 1, pp. 183-197.

ABSTRACT

Although finite element packages facilitating coupled consolidation analyses are increasingly in use, many practitioners still favour linear uncoupled analysis out of familiarity with the use of coefficients of consolidation. However, coefficients of consolidation measured by any single means tend to exhibit significant variation, with mean results from different laboratory and field tests also varying widely, leaving uncertainly over the correct values to apply to field problems. In this paper, a finite difference approach is used to back-calculate operational coefficients of consolidation from pore pressure measurements pertinent to a pile group driven in clay-silt. The research shows that this method is capable of successfully capturing the process of pore pressure dissipation, and that the operational coefficient of consolidation around the pile group is higher than that derived from piezocone dissipation tests in the same material.

1. INTRODUCTION

An assessment of the settlement rate of foundations or embankments constructed on fine-grained soils is often hampered by uncertainty over the correct choice of consolidation parameters, c_v and c_h, the vertical and horizontal coefficients of consolidation respectively. Significant theoretical advances (e.g. Baligh and Levadoux 1986, Houlsby and Teh 1988) have meant that c_h values interpreted from piezocone dissipation tests are regarded as more reliable than those determined in the laboratory, such as from oedometer or Rowe Cell tests. However, Lunne *et al.* (1997) warn that c_h determined from piezocone dissipation tests will only be accurate to within half an order of magnitude. The state of overconsolidation is also very relevant; data from Leroueil and Hight (2003), for example, suggest that c_h measured in dissipation tests with low to moderate overconsolidation ratios is approximately the geometric mean of the normally and overconsolidated values (Lehane *et al*., 2009). Robertson *et al.* (1992) have also highlighted scale effects in field values of c_h; a piezocone with cross-sectional area of 15 cm^2 was found to yield values of c_h that were 50% higher than that from a piezocone with cross-sectional area of 10 cm^2.

Other *in situ* tests have also been used; Chu *et al*. (2002) compares c_h values for Singapore marine clay determined by a piezocone (2-4 m^2/year), flat dilatometer (1-5 m^2/year) and self-boring pressuremeter (2.5-20 m^2/year), all of which overestimate c_h backfigured from vertical drains in the field (0.7-1.2 m^2/year, Bo *et al.*, 1997). Totani *et al.* (1998) also report discrepancies between c_h values determined using different dilatometer types in fine-grained Italian soils.

In addition, the ratio of c_h/c_v is also relevant to some geotechnical problems (it may guide the spacing of prefabricated vertical drains, for example) and inherent anisotropy causes the ratio to vary considerably. Our understanding of these anisotropic effects is not helped by the fact that ratios of c_h/c_v reported in the literature often have had c_h and c_v determined by different means and at different states of overconsolidation. Totani *et al.* (1998) report values of c_h/c_v typically between 1 and 4 showing dependence on soil type,

but also on the methods used. Ratios of c_h/c_v as high as 10 have been reported elsewhere in the literature (e.g. Levadoux and Baligh 1986, Robertson *et al.* 1992, Look 2007). Interestingly, Levadoux and Baligh (1986) conclude, from studies using the Strain Path Method, that c_h is the dominant driver of dissipation around a penetrometer, with c_h/c_v having little effect on pore pressure dissipation.

In this paper, a backanalysis of pore pressure measurements made following the installation of a group of piles in a lightly overconsolidated clay-silt is conducted. This backanalysis employs linear consolidation theory with the objectives of (a) verifying the general applicability of this approach for the assessment of pore pressure dissipation around pile groups and (b) determining the applicability of c_h values derived from piezocone dissipation tests for such problems. Although fully coupled consolidation analyses are now relatively common, the analyses presented here employs linear consolidation theory in view of its continued popularity; such popularity stems from practitioners' experience in the use and application of coefficients of consolidation. Soderberg (1962) has explored a similar finite difference approach, but has assumed a constant c_h with time, whereas a continuous change in c_h with time has been modelled in this study. Axisymmetric finite element analyses, modelling installation using a cylindrical cavity expansion process, have also been used as a check on initial pore pressure measurements.

2. BACKGROUND TO SITE AND GROUND CONDITIONS

2.1 Geotechnical conditions

The pore pressure measurements interpreted in this paper pertain to a programme of full-scale pile group testing at a geotechnical test bed near Belfast, Northern Ireland reported by McCabe and Lehane (2003, 2006a, 2008). The stratigraphy close to ground level comprised 1m of topsoil interbedded with gravel fill overlying 0.7m of medium dense fine grained organic silty sand. The 6m long test piles were embedded primarily in a layer of soft, estuarine, lightly overconsolidated clay-silt (known locally as *sleech*) that extended from a depth of 1.7m to ≈ 9m below ground level. The *sleech* is found to plot

exactly on the A-line of the BS5930 plasticity chart based on its liquid and plastic limits. Summary properties of this material are provided in Table 1. The groundwater level varied both seasonally and tidally within the range 1.0m - 1.3m below ground level.

Average values of C_c (the normally consolidated compression index of the *sleech* up to a vertical effective stress of 1 MPa) and e_0 (the initial void ratio) were found to be 0.60 and 1.73 respectively. Measured compression indices for the reconstituted soil (C_c*) were in close agreement to those deduced from Burland's (1990) correlation between C_c* and the void ratio at the liquid limit e_L (i.e. $C_c^* = 0.256e_L - 0.04$). Use of this correlation for all oedometer tests indicated a relatively constant C_c/C_c^* ratio of 1.3 ± 0.1.

Variations in oedometer c_v with stress level are shown in Figure 1a, with permeabilities (k) inferred from the same set of tests shown in Figure 1b. Values of c_v reduced from typically 0.8 m^2/year or higher in the overconsolidated region to about 0.4 m^2/year at a vertical effective stress of 100kPa.Values of k reduce with increased stress levels but typically lie in the range 1.5×10^{-10} m/s to 5×10^{-10} m/s at *in situ* stress levels. In spite of the high silt content, the k and c_v values are more typical of a clay than a silt and highlight the influence of the clay fraction. Three piezocone dissipation tests were carried out in the *sleech* at depths between 2.5m and 5.5m. Values of c_h were interpreted using the Houlsby and Teh (1988) procedure to fall in the range 7-12 m^2/year.

2.2. Pile group and piezometers

The pile group configuration, shown in Figure 2, comprised 250mm (=B) square precast concrete piles, with a 'centre' pile installed first followed by four equally spaced 'corner' piles, with a centre to corner spacing to pile width ratio (s/B) of 2.8 ± 0.1. In each case, only one or two hammer blows (5 tonne weight, 0.45m drop height) were required to penetrate the fill, with the self-weight of the hammer itself sufficient thereafter to push the pile to its final embedment length of 6.0m.

A total of nine pneumatic piezometers were installed at various depths (z) and radial distances (r) around the planned position of pile group G2 to measure installation pore

pressures (Table 2). The piezometer locations have also been included in Figure 2 (with the exception of piezometers 8 and 9, which are located at a significant radial extent from the group centre). The piezometer readings were recorded until 43 days after installation of the group. As noted by McCabe and Lehane (2006a), temporary increases in pore pressure could not be accurately monitored because of the manual (and hence slow) nature of the pore pressure recording system employed at the site.

3. PORE PRESSURE MEASUREMENTS

The maximum excess pore pressure ratio (u_e/σ'_{vo}; where u_e is the maximum excess pore pressure and σ'_{vo} is the free-field vertical effective stress) derived from piezometer measurements is plotted as a function of radial distance from the pile group centre normalised by the width of one pile (r/B) in Figure 3. For those piezometers at depths shallower than pile base level and beyond r/B=2.5, u_e/σ'_{vo} varies approximately linearly with the logarithm of r/B, while a lower value was registered at the single piezometer location below the pile base. McCabe and Lehane (2006a) compare these data with corresponding data for single piles in clay to show that the excess pore pressure field around a pile group has both greater magnitude and radial extent than the field around a single pile, supporting earlier findings for a group of 116 concrete piles installed in marine clay reported by Bozozuk *et al.* (1978). In Figure 4, the apparent degree of dissipation U ($=u_t/u_e$; where u_t is the excess pore pressure at any time) is plotted as a function of the logarithm of time for six piezometers. The curves are consistent and indicate that the excess pore pressures generated by driving have dissipated considerably (but not completely) after 43 days. However, these data are uncorrected for a small seasonal rise in water table of 0.1-0.2m (noted in a local standpipe over the dissipation period) and therefore the real extent of dissipation will be greater, especially for those piezometers registering lowest u_e values. The initial dissipation at piezometer 1, which is at a significant distancefrom the pile group centre plotted on Figure 2, shows slower dissipation initially than at the other locations.

The closest piezometer to the centre group pile, piezometer 6, was positioned between two corner piles at r/B=3. Although there were no pore pressure sensors on the centre pile itself, it has been possible to infer maximum excess pore pressures at the centre pile shaft from peak installation total stresses recorded on the centre pile over the course of group installation (McCabe and Lehane, 2006a). Assuming that horizontal effective stresses during installation are no larger than $\approx 0.2\sigma'_{vo}$ (Lehane *et al.,* 1994), values of u_e/σ'_{vo} = 3.1 and 2.7, at 5.25m and 3.25m depth respectively, may be inferred and are included on Figure 3 at r/B = 0.5. The inferred pore pressures in the model are not particularly sensitive to the coefficient of σ'_{vo} assumed in the range 0-0.2. These values are also in keeping with u_e/σ'_{vo} values on the centre pile of a model pile group of the same configuration , reported by McCabe *et al.* (2008).

4. 3-D LINEAR UNCOUPLED CONSOLIDATION THEORY

The consolidation process may be described by eqn. [1] for problems exhibiting radial symmetry (Barron, 1948):

$$\frac{\delta u_e}{\delta t} = c_v \frac{\partial^2 u_e}{\partial z^2} + c_h \left(\frac{\partial^2 u_e}{\partial r^2} + \frac{1}{r} \frac{\partial u_e}{\delta r} \right) \qquad [1]$$

where t is time and z is depth. Eqn. [1] may be solved using a Central Difference approach, by approximating the derivative terms according to eqns. [2a]-[2d]. The schematic in Figure 5 may be used to understand the relevance of the subscripts to the u_e values; the first subscript (0,1,2,3 or 4) represents position in r-z space while the second represents time steps in the consolidation process (time step from k to k+1 shown). Note that the subscript ‘e’ (denoting that these pore pressures are excess values) are omitted from the finite difference terms on the right of the relevant equations for clarity.

$$\frac{\delta u_e}{\delta t} = \frac{u_{0,k+1} - u_{0,k}}{\Delta t} \qquad [2a]$$

$$\frac{\delta^2 u_e}{\delta z^2} = \frac{u_{2,k} + u_{4,k} - 2u_{0,k}}{\Delta z^2} \quad [2b]$$

$$\frac{\delta^2 u_e}{\delta r^2} = \frac{u_{1,k} + u_{3,k} - 2u_{0,k}}{\Delta r^2} \quad [2c]$$

$$\frac{\delta u_e}{\delta r} = \frac{u_{3,k} - u_{1,k}}{2\Delta r} \quad [2d]$$

The solution is given in eqn. [3] for the situation where the increments of depth and radial distance are equivalent (i.e. $\Delta z = \Delta r = h$):

$$u_{0,k+1} = u_{0,k}\left(1 - 2\beta_v\left(1 + \Omega\right)\right) + \Omega\beta_v\left(u_{1,k}\left(1 - \frac{h}{2r}\right) + u_{3,k}\left(1 + \frac{h}{2r}\right)\right) + \beta_v\left(u_{2,k} + u_{4,k}\right) \quad [3]$$

$$\Omega = \frac{\beta_h}{\beta_v} = \frac{c_h}{c_v} \quad [3a]$$

$$\beta_v = \frac{c_v \Delta t}{h^2} \quad [3b]$$

$$\beta_h = \frac{c_h \Delta t}{h^2} \quad [3c]$$

At the radial origin (r=0) or axis of symmetry, the condition in eqn. [4a] holds, and with no flow across this symmetry boundary, $u_{3,k} = u_{1,k}$, eqn. [4b] is used instead of eqn. [3]:

$$\frac{1}{r}\frac{\delta u_e}{\delta r} \rightarrow \frac{\delta^2 u_e}{\delta r^2} \quad [4a]$$

$$u_{0,k+1} = u_{0,k}\left(1 - 2\beta_v\left(1 + 2\Omega\right)\right) + \beta_v\left(u_{2,k} + u_{4,k} + 4\Omega u_{3,k}\right) \quad [4b]$$

An initial distribution of pore pressures (at t = 0) is required to start the iterative process described above. In addition, combinations of Δt and h values are constrained to ensure that β_v and β_h are no greater than 1/6, required for stability of eqns. [3] and [4b] (e.g. Scott, 1963).

5. INITIAL PORE PRESSURES AND FINITE DIFFERENCE COMPUTATIONS

5.1 Initial Pore Pressure Distribution

Two independent estimates of the maximum excess pore pressure field (u_e) around the pile group, for subsequent use as the starting datasets for eqns. [3] and [4], were obtained as follows:

5.1.1 Contour map based on measured pore pressures

An approximate hand-drawn contour map of u_e/σ'_{vo} values in r-z space was developed based upon the datapoints shown in Figure 3. An interpolation/extrapolation approach, guided by the example of an excess pore pressure field around a piezocone (Levadoux and Baligh, 1986) was used to populate the contour map to a radial distance from the pile group centre of 48B = 12m and over the depth range 2.0m to 9.0m depth (i.e. 12B beneath the level of the pile base) within the *sleech*. A grid of initial excess pore pressures (u_e) at vertical and radial spacings of 0.5m (= $\Delta z = \Delta R = h$) was then extracted from this map (plotted in Figure 6) for the finite difference model.

5.1.2 PLAXIS 2D Analysis

It is acknowledged that a 3D analysis would be required to capture the discrete geometry of the piles in a 5-pile group, as well as the positions of those piezometers (3 and 6) located within the group perimeter. However, in this case a simplified 2D (axisymmetric) model is used merely as a general check on the suitability of the contour map in Figure 6. Clancy and Randolph (1996) and Horikoshi and Randolph (1999) have each described two cases where a pile group has been approximated as an equivalent single 'pier', based on the approach illustrated by Poulos and Davis (1980).

On this basis, a PLAXIS 2D (Brinkgreve *et al.*, 2010) analysis was carried out with the pile group modelled as a single pile of equivalent cross sectional area to the five group piles (i.e. pile radius $R_g = B(5/\pi)^{0.5} \approx 0.32$m). The pile material was set as linear elastic and non-porous with a Young's Modulus of 30 GPa, a Poisson's ratio of 0.15 and a unit weight of 24 kN/m^3. However, since the pile is really only a mechanism to generate the

cavity expansion, the exact values are of little consequence (Guetif *et al*. (2007) provides further information on the use of 'dummy' piles). The pore pressures were generated by applying a cylindrical cavity expansion to a final pile radius of R_g. The effect of varying the initial radius a (where $a<R_g$) was examined; the authors considered the work of Carter *et al.* (1979) who found that the doubling of a cavity radius (i.e. $R_g/a=2$) is sufficient to give an adequate approximation of what happens in a soil when modelling the installation of a pile. The main effect of an expansion beyond twice the initial radius is merely to cause a further growth of the annular region of yielded soil.

Mesh and boundary sensitivity analyses were carried out and the mesh was refined close to $r=R_g$ where the largest strains resulting from the cylindrical cavity expansion process were anticipated. The final mesh, consisting of approximately 4500 15-node triangular elements, is shown in Figure 7. The hyperbolic elastoplastic Hardening Soil constitutive model in PLAXIS was used to model the behaviour of the fill, *sleech* and silty sand; the parameters adopted have been developed for this work based upon data from McCabe (2002) and McCabe and Lehane (2006b) and are shown in Table 3.

A value of m=1, where m dictates the amount of stress dependency, has been selected for the *sleech* in order to simulate logarithmic compression behaviour (e.g. Brinkgreve *et al.*, 2010) while a value of m = 0.5 has been used for the stiffer fill and sand layers as suggested by Janbu (1963). The secant modulus (E_{50}^{ref} = 25MPa) for the fill at a reference pressure (p_{ref}) of 30kPa was selected based on analyses carried out by McCabe and Lehane (2006b) in OASYS SAFE. A lower secant modulus (E_{50}^{ref} = 9MPa) has been used for the *sleech* layer. A cohesion of 0.5kPa has been used universally for numerical stability purposes (e.g. Killeen and McCabe, 2010).

The PLAXIS 2D 'Soil Test' facility has been used to simulate 54mm diameter K_0 consolidated triaxial compression (CK_0UC) tests carried out on *sleech* samples where the in-situ stress state was reinstated by consolidation and swelling to artificially induce the required level of overconsolidation (McCabe, 2002). Small strain shear stiffness values, G_{sec} (calculated from E_{sec} with $\nu = 0.5$ for undrained conditions) normalised by the initial

mean effective stress at the beginning of undrained shearing, p'_0, reported by McCabe (2002) have been compared to PLAXIS output (Figure 8a). The corresponding stress paths in p'-q space are also compared in Figure 8b. The reasonable agreement (with slight deviation at high strains for the case of G_{sec}/p'_0) obtained gives confidence in the model parameters.

The *Undrained A* approach (effective strength and stiffness parameters) in PLAXIS has been used to define the soil parameters. It is therefore necessary to ensure the model predicts the correct undrained shear strength (representative of actual field conditions). The undrained shear strength profile with depth has been validated by comparison with measured undrained shear strengths from shear vane tests carried out by McCabe (2002), see Figure 9. Correction factors (based on the plasticity index, I_p) documented by Bjerrum (1972) have been applied to the measured values. A reasonable match is obtained, although it is acknowledged that the gradient with depth is somewhat steeper in the field.

The cavity expansion process was simulated in undrained conditions as a prescribed displacement from an initial radius (a) to a final radius (R_g). The application of a prescribed displacement in this manner was deemed to be the best option for numerical stability purposes (Kirsch 2006, Castro and Karstunen 2010), as opposed to the application of a volume strain to an expanding soil cluster.

5.1.3 Comparison of two approaches for initial pore pressures

The u_e distributions developed from the approaches in sections 5.1.1 and 5.1.2 are plotted against r in Figure 10 for three different horizontal planes (at depths of 3m, 4m and 5m), all above pile base level. It can be observed that:

(i) The PLAXIS-generated solutions are relatively insensitive to the choice of R_g/a for the three values in the range 1.58 to 3.15 considered.

(ii) Given the limitations of the 2D equivalent single pile analysis described, the match between PLAXIS and contour map profiles is reasonably good, and importantly at the pile-soil interface.

However, close to and beneath pile base level, where a spherical cavity expansion process is more relevant that a cylindrical one, the methods deviate as expected. Given the agreement between the two distributions above ≈ 6m (pile tip) where the cavity expansion approach is applicable, it was deemed appropriate to use the initial contour plot to give a complete set of u_e values over the field being modelled.

Levadoux and Baligh (1986) and Robertson *et al.* (1992), describing the consolidation process around a piezocone, have indicated that calculated pore pressures are sensitive to the initial distribution assumed around the piezocone. However, sensitivity analyses conducted as part of this research have suggested that pore pressure predictions beyond 1m from the pile group centre (r/B = 4) were relatively insensitive to the initial pore pressure distribution close to the pile group centre and have little bearing on subsequent conclusions.

5.2 Pore Pressure Dissipation using the Finite Difference Formulation

The initial u_e distribution, on which Figure 6 is based, was entered on a spreadsheet and the pressures at subsequent time intervals were calculated on subsequent tabs using eqns. [3] and [4b] while observing conditions of free drainage (u = 0) at top, bottom and far radial boundaries. In order to meet convergence criteria for β_h (eqn [3b]) and anticipating that c_h values up to 1000 m^2/year may be used, a small time interval of Δt = 0.375 hours (requiring 43 days × 64 tabs/day = 2752 sheets in MS Excel) was preferred to a low h value (i.e. a tighter grid) given the limited data available to develop the initial pore pressure contour plot.

The origin of the pore pressure field is at R=0 and therefore the pile has not been included discretely in the finite difference model (this is apparent from Figure 10). However, the sensitivity analysis alluded to in section 5.1.3 gives confidence that this assumption does not unduly affect the predictions.

6. RESULTS AND DISCUSSION

6.1 Effect of c_h/c_v ratio

Preliminary studies indicated that the overall degree of dissipation at 43 days was modelled reasonably well by assuming c_h = 50 m^2/year, although the predictions at all intermediate stages of dissipation were unsatisfactory. However, c_h = 50 m^2/year was fixed for a preliminary study to assess the effect of varying the c_h/c_v ratio. Four different values, c_h/c_v = 1, 2, 5 and 10 spanning the range encountered in the literature, are shown in Figures 11a-11f. These figures indicate that the effect of varying c_h/c_v is not negligible. However, it was not possible to have both c_h and c_h/c_v as variables in this exercise, so the less sensitive c_h/c_v value is hereafter fixed at 2, a reasonable compromise from values reported in the literature for similar materials.

6.2. Selecting appropriate c_h values

Any change in c_h over time will be related to changes in stress level and OCR and will be continuous rather than stepwise. During pile installation, the effective stresses in the ground approach zero and the OCR increases significantly; the permeability and c_h increases in response. After u_e has been reached, the effective stresses recover and OCR reduces with a corresponding reduction in permeability and c_h. For the purposes of this analysis, the authors have considered this post-driving reduction of c_h with time in a sufficient number of steps to give an adequate match to the pore pressure-time plots.

Best fits between measurements and predictions for piezometers 1, 2, 4, 5, 6 and 7 are shown in Figure 12a-12f, labelled with the notional c_h steps used to achieve the fit. The following observations can be made:

- The fits achieved in Figure 12 are considerably better than those in Figure 11 (which were based on a single c_h value). In particular, the predictions for piezometers 1 and 7 (Figures 12e and 12f) are much more representative of the data than those in Figures 11e and 11f.

- c_h values in the range 100-1000 m^2/year are required for the predictions to match the measurements for the 2 day period immediately after u_e was reached. These values are quite high in relation to the oedometer c_v values, but are temporary and are likely to reflect the significant changes in effective stress during this period.
- Highest early $c_h$values pertain to those piezometers furthest from (piezometers 1 and 7) or below (piezometer 5) pile base level, perhaps reflecting the more 3-D nature of drainage in these areas. Piezometers 2, 4 and 6 which are well above the pile tip, show similar c_h values over the first 2 days; fastest dissipation is registered for Piezometer 6 closest to the pile group centre (r/B=3).
- The high short-lived c_h values reduce considerably with time, ultimately returning to consistent values of $c_h \approx$ 20-30 m^2/year for most piezometers towards the end of the dissipation period. In the case of piezometers 1 and 2, no attempt has been made to interpret a c_h value for the end of the dissipation period as these data are by then affected by the aforementioned seasonal water table rise more than by the pile group.

6.3 Discussion

It is apparent from Section 6.2 that, close to the pile group, c_h reduces as radial effective stresses in the ground increase during equalization. The inferred value corresponding to the latter part of equalization, c_h = 20-30 m^2/year, is higher by a factor of ≈2.5 than the values derived from piezocone tests (7-12m^2/year) at equivalent depths. This seems to confirm the existence of a scale effect on c_h, with considerably higher values relevant to a 625cm^2 pile base than a 10cm^2 60^0 CPT cone. While the aforementioned c_v and k values measured in standard oedometer tests were suggesting a highly influential clay fraction, the c_h values inferred from the modelling exercise in this paper are more compatible with the high silt content. It is also noteworthy that the average field value of c_h at the well-researched Bothkennar Carse Clay site, appropriate to 50.8mm diameter jacked single piles is 30m^2/year, which is not much lower than the average value of 50m^2/year mentioned in Section 6.1.

7. CONCLUSIONS

In this paper, pore pressure measurements around a pile group in clay/silt have been used to backcalculate c_h values during the dissipation period and put them in the context of c_h determined by oedometer and piezocone dissipation testing. The following conclusions can be drawn from the exercise:

a) A suitable stepwise reduction in c_h with time, used in conjunction with linear uncoupled consolidation theory, appears to be an effective method of predicting the excess pore pressure dissipation generated around a pile group driven in Belfast *sleech*. It is apparent that these changes in c_h with time are generated by changes in stress level and the overconsolidation ratio of the ground owing to pile installation.
b) Initial c_h values, over the first couple of days of dissipation lie in the range of 100-1000 m^2/year and far exceed what might be expected from piezocone dissipation tests. These transient values appear to show some dependence on depth and/or position relative to the pile base.
c) Values of c_h towards the end of dissipation period tend to lie in the range 20-30 m^2/year, approximately greater than piezocone-inferred values by a factor of 2.5. This seems to justify the existence of a scale effect on c_h values.

ACKNOWLEDGEMENTS

The second author would like to acknowledge the support of the Irish Research Council for Science, Engineering, and Technology (IRCSET) for supporting his research work at NUI Galway.

REFERENCES

Baligh MM, Levadoux JN (1986) Consolidation after Undrained Piezocone Penetration. II: Interpretation. Journal of Geotechnical Engineering 112(7): 727-745.

Barron (1948) Consolidation of fine-grained soils by drain wells. Transactions of ASCE 113: 718-742.

Bjerrum L (1972) Embankments on soft ground. Proceedings of the ASCE Specialty Conference on Performance of Earth and Earth-Supported Structures, Purdue University, 2: 1-54.

Bo MW, Arulrajah A, Choa V (1997) Performance verification of soil improvement work with vertical drains. Proceedings of the 30th Anniversary Symposium of the Southeast Asian Geotechnical Society, Bangkok, Thailand, 191-203.

Bozozuk M, Fellenius BH, Samson L (1978) Soil disturbance from pile driving in sensitive clay. Canadian Geotechnical Journal 15(3): 346-361.

Brinkgreve RBJ, Swolfs WM, Engin E (2010) PLAXIS 2D 2010 Finite Element Code, PLAXIS B.V., The Netherlands.

British Standard 5930 (1999). Code of Practice for Site Investigations. British Standards Institution, London.

Burland JB (1990) On the compressibility and shear strength of natural clays. Géotechnique 40(3): 329-378

Carter JP, Randolph MF, Wroth CP (1979) Stress and pore pressure changes in clay during and after the expansion of a cylindrical cavity. International Journal for Numerical and Analytical Methods in Geomechanics 3(4): 305-322.

Castro J, Karstunen M (2010) Numerical simulations of stone column installation. Canadian Geotechnical Journal 47(10): 1127-1138.

Chu J, Bo MW, Chang MF, Choa V (2002) Consolidation and Permeability Properties of Singapore Marine Clay. Journal of Geotechnical and Geoenvironmental Engineering 128(9): 724-732.

Clancy P, Randolph MF (1996) Simple design tools for piled raft foundations. Géotechnique 46(2): 313-328.

Guetif Z, Bouassida M, Debats JM (2007) Improved soft clay characteristics due to stone column installation. Computers and Geotechnics 34(2): 104-111.

Horikoshi K, Randolph MF (1999) Estimation of overall settlement of piled rafts. Soils and Foundations 39(2): 59-68.

Houlsby GT, Teh CI (1988) Analysis of the piezocone in clay. Proceedings of the International Symposium on Penetration Testing, Rotterdam, the Netherlands, 1: 777-783.

Janbu N (1963) Soil compressibility as determined by oedometer and triaxial tests. Proceedings of the European Conference on Soil Mechanics and Foundation Engineering, Wiesbaden, 1: 19-25.

Killeen MM, McCabe BA (2010). A numerical study of factors governing the performance of stone columns supporting rigid footings on soft clay. Proceedings of the 7th European Conference on Numerical Methods in Geotechnical Engineering, Trondheim, Norway, 833-838.

Kirsch F (2006) Vibro stone column installation and its effect on ground improvement. Proceedings of the International Conference on Numerical Simulation of Construction

Processes in Geotechnical Engineering for Urban Environment, Bochum, Germany, 11-124.

Lehane BM, Jardine RJ, Bond AJ, Chow FC (1994) The development of shaft friction on displacement piles in clay Proceedings of the 13th International Conference on Soil Mechanics and Foundation Engineering, New Delhi, 473-476.

Lehane BM, O'Loughlin CD, Gaudin C, Randolph MF (2009) Rate effects on penetration resistance in kaolin. Géotechnique 59(1): 41-52.

Leroueil S, Hight DW (2003) Behaviour and properties of natural soils and soft rocks. Proceedings of the Symposium on Characterisation and Engineering Properties of Natural Soils, Singapore, 1: 29-254

Levadoux JN, Baligh MM (1986). Consolidation after UndrainedPiezocone Penetration. I: Prediction. Journal of Geotechnical Engineering 112(7): 707-726.

Look BG (2007) Handbook of Geotechnical Investigation and Design Tables, Taylor and Francis, London.

Lunne T, Robertson PK, Powell JJM (1997) Cone Penetration Testing in Geotechnical Practice, Blackie Academic/Chapman and Hall, E&FN Spon, London.

McCabe BA Lehane BM (2003) Stress changes associated with driving pile groups in clayey silt, Proceedings of the 13th European Conference of Soil Mechanics and Geotechnical Engineering, Prague, 2: 271-276.

McCabe BA (2002) Experimental investigations of driven pile group behaviour in Belfast soft clay. PhD Thesis, University of Dublin, Trinity College.

McCabe BA, Gavin KG, Kennelly M (2008) Installation of a reduced-scale pile group in silt. Proceedings of the 2nd British Geotechnical Association International Conference on Foundations, Dundee, 1: 607-616.

McCabe BA, Lehane BM (2006a) Behavior of Axially Loaded Pile Groups Driven in Clayey Silt. Journal of Geotechnical and Geoenvironmental Engineering 132(3): 401-410.

McCabe BA, Lehane BM (2006b) Prediction of pile group response using a simplified non-linear finite element model. Proceedings of the 6th European Conference on Numerical Methods in Geotechnical Engineering, Graz, Austria, 589-594.

McCabe BA, Lehane BM (2008) Measured and predicted t-z curves for a driven single pile in lightly overconsolidated silt. Proceedings of the 3rd International Conference on Site Characterization, Taipei, 487-491.

McCabe BA, Killeen MM, Egan D (2008) Challenges faced in 3D finite element modeling of stone column construction. Proceedings of the Joint Symposium on Concrete Research and Bridge Infrastructure Research in Ireland, Galway, 393-400.

Poulos HG, Davis EH (1980) Pile Foundation Analysis and Design, John Wiley & Sons, New York.

Robertson PK, Skully JP Woeller DJ, Lunne T, Powell JJM, Gillespie DG (1992) Estimating coefficient of consolidation from piezocone tests. Canadian Geotechnical Journal 29(4): 539-550.

Scott RF (1963) Principles of soil mechanics, Addison Wesley, Reading, Mass.

Soderberg LO (1962) Consolidation Theory Applied to Foundation Pile Time Effects. Géotechnique 12(3): 217-225.

Totani G, Calabrese M, Monaco P (1998) In situ determination of c_h by flat dilatometer (DMT). Proceedings of the First International Conference on Site Characterization, ISC '98. Atlanta, Georgia (USA), 2: 883-888.

Figure 1: Variations in oedometer c_v and permeabilities (k) with stress level

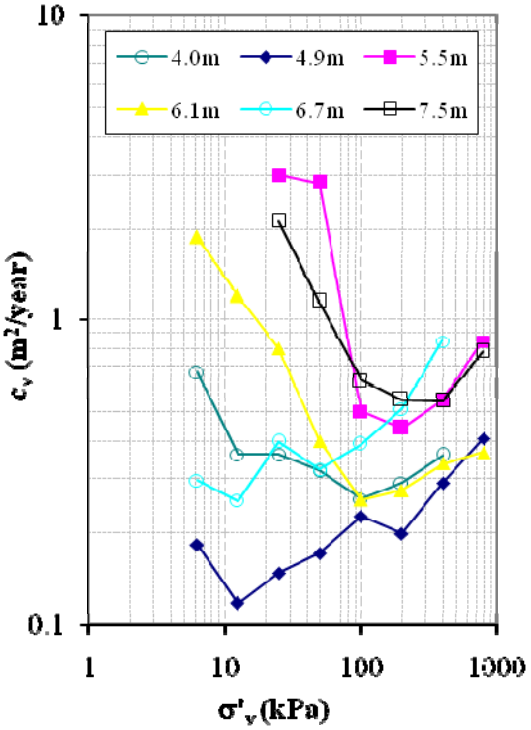

1a: Oedometer c_v with stress level

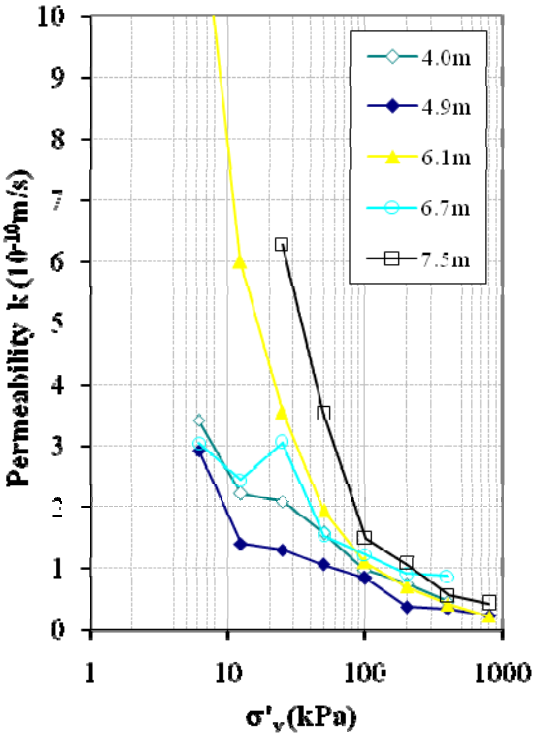

1b: Permeability (k) with stress level

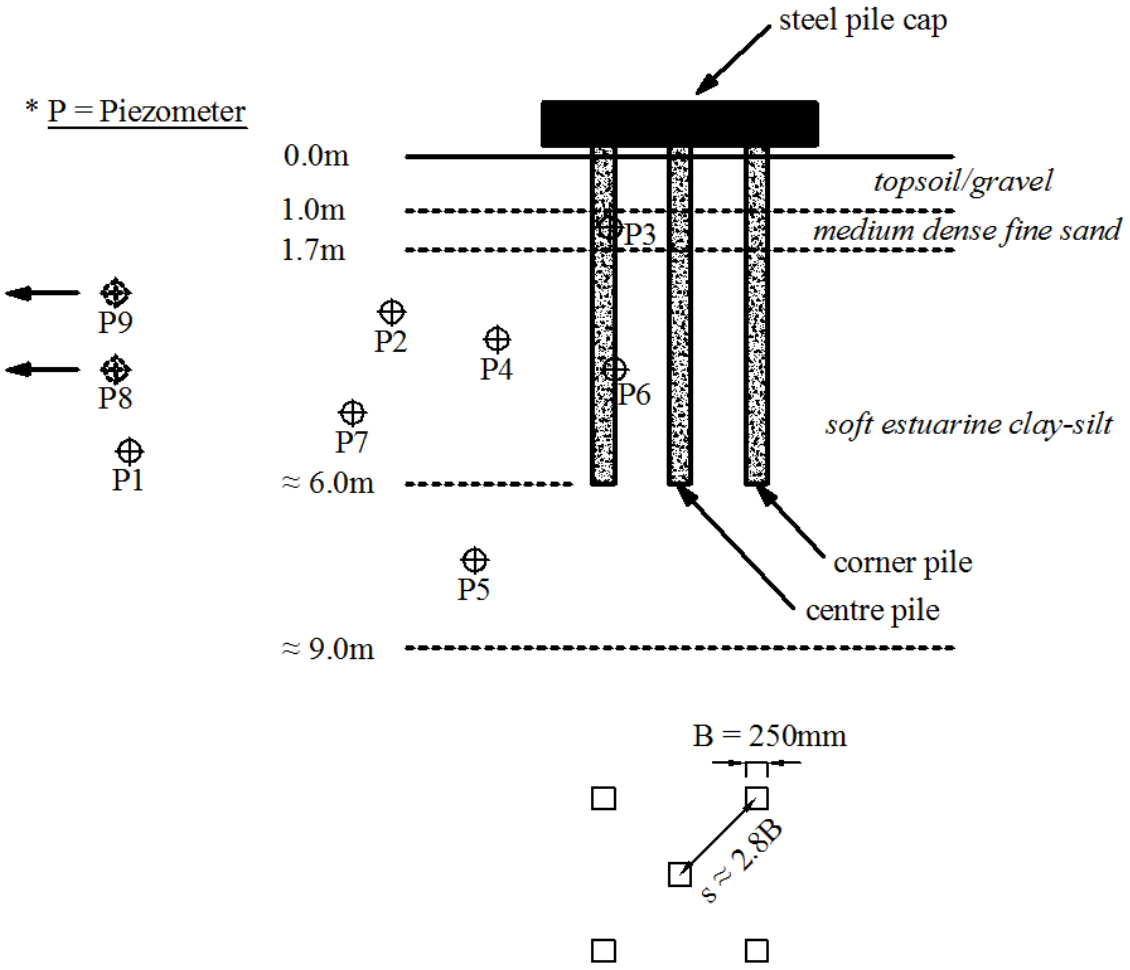

Figure 2: Pile Group Configuration

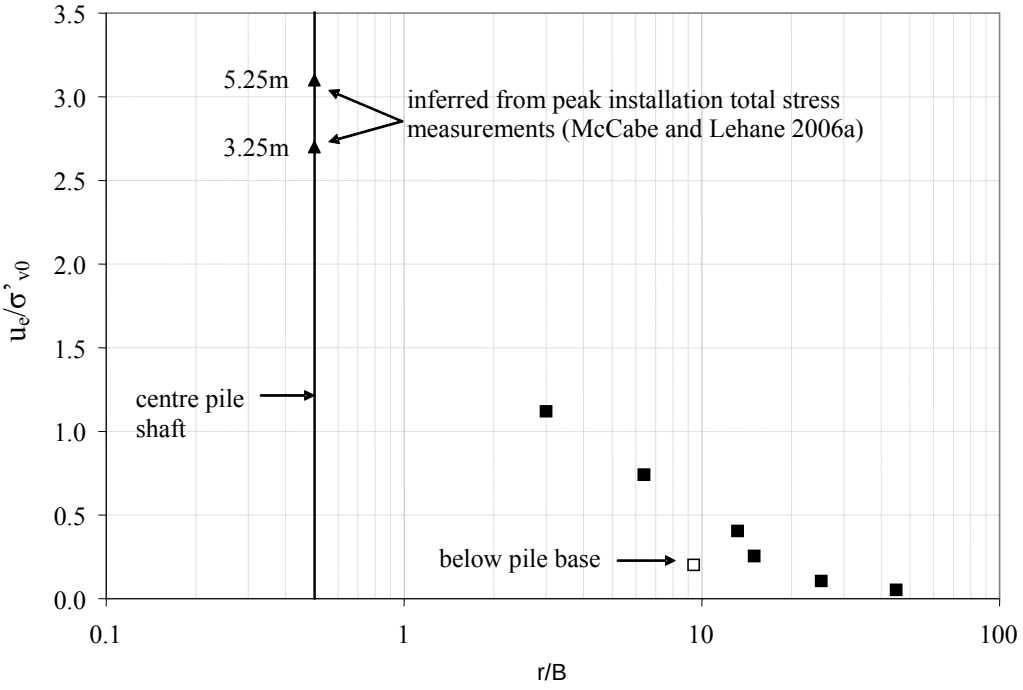

Figure 3: Maximum excess pore pressure around pile group G2

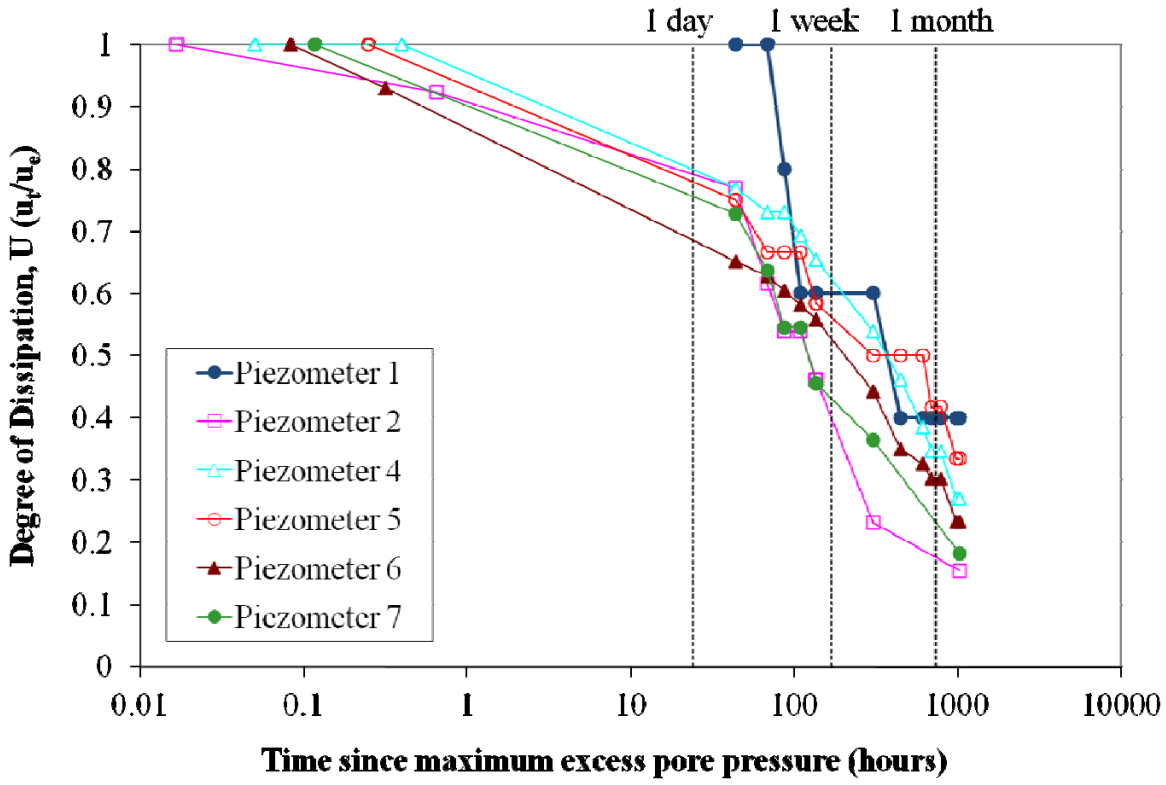

Figure 4: Degree of dissipation versus time for piezometers

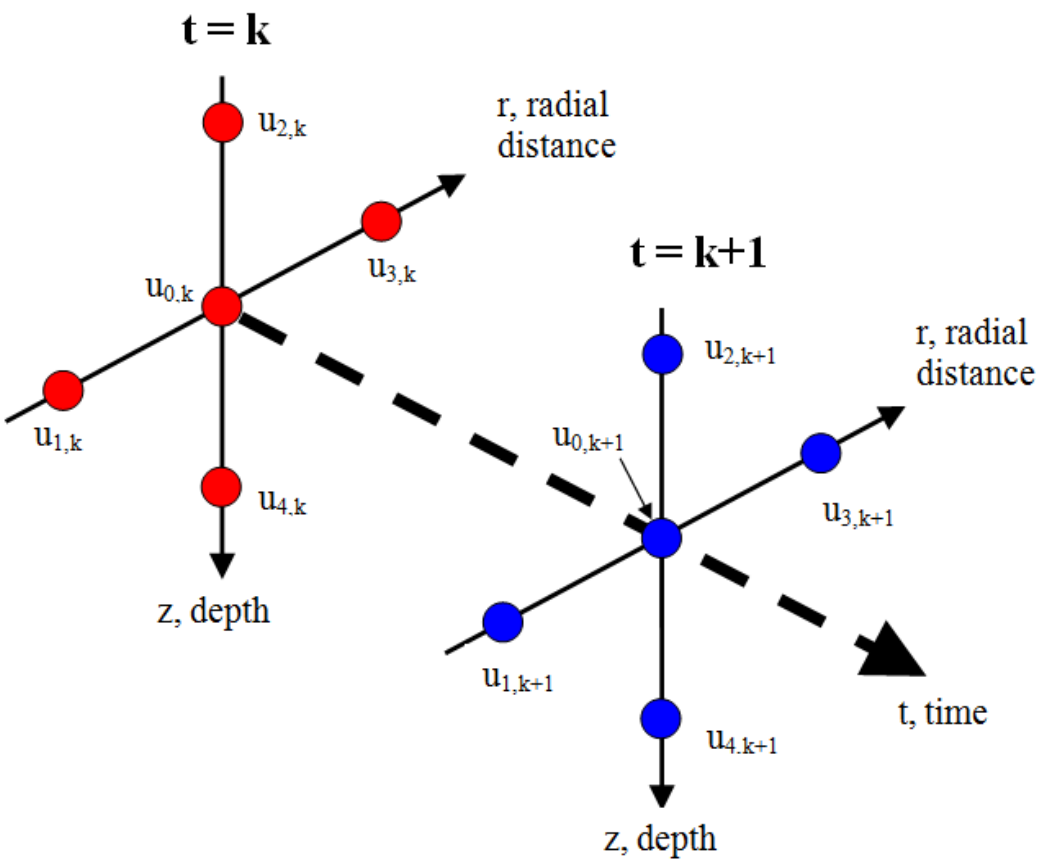

Figure 5: Schematic of Central Difference Formulation

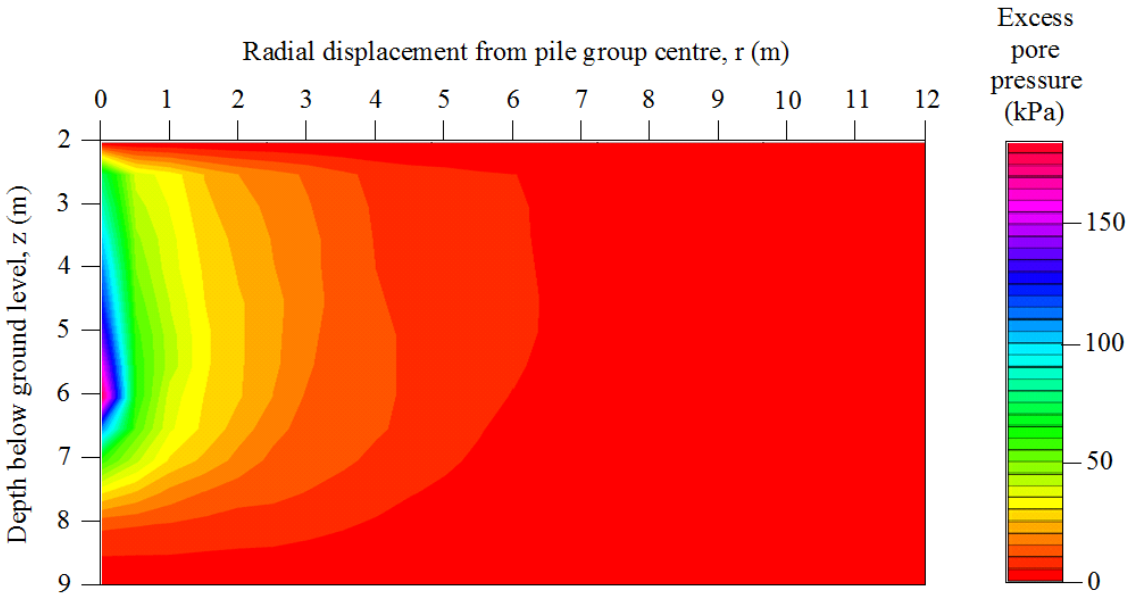

Figure 6: Initial u_e distribution (at t = 0)

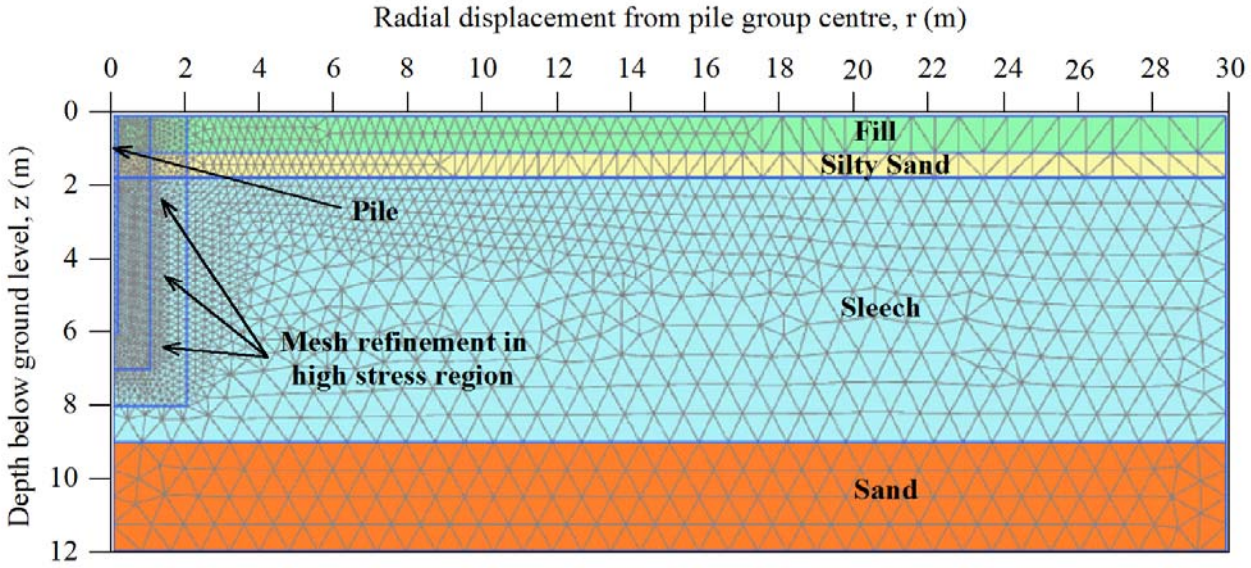

Figure 7: Finite Element Mesh

Figure 8: Comparison with CK_0UC tests reported by McCabe (2002)

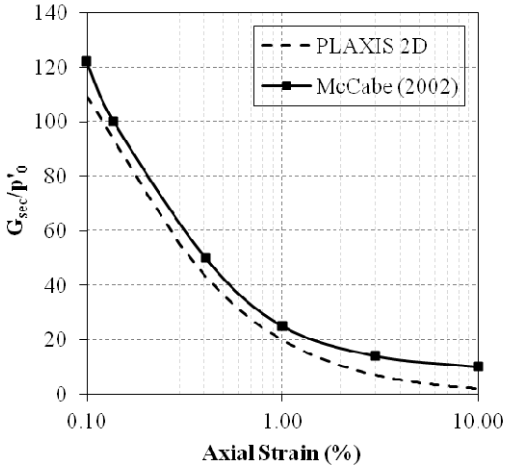

8a: G_{sec}/p'_0 versus Axial Strain

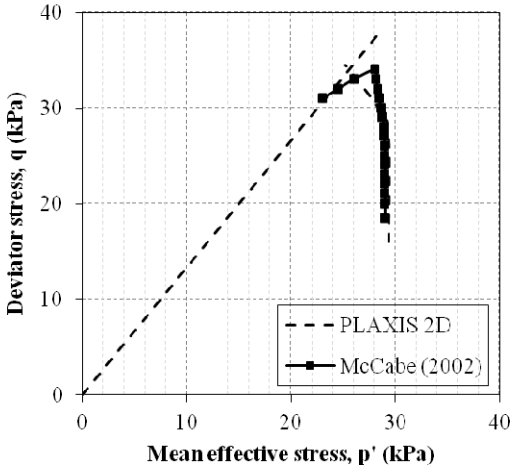

8b: Stress paths in p'-q space

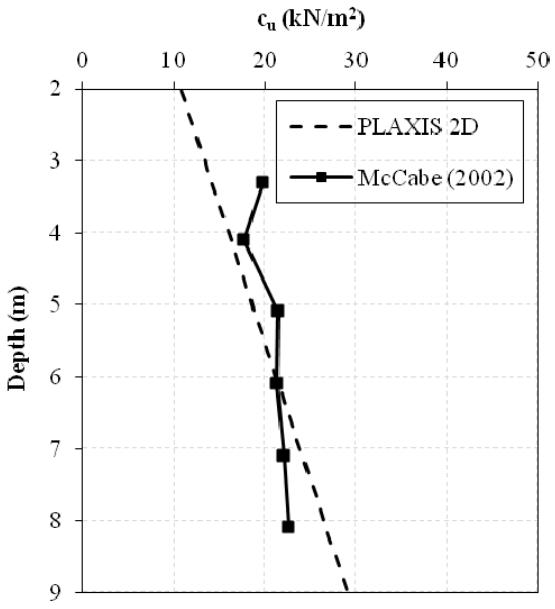

Figure 9: Comparison of undrained shear strength profile with McCabe (2002)

Figure 10: Comparison between the contour-map and PLAXIS-generated u_e distributions at different depths

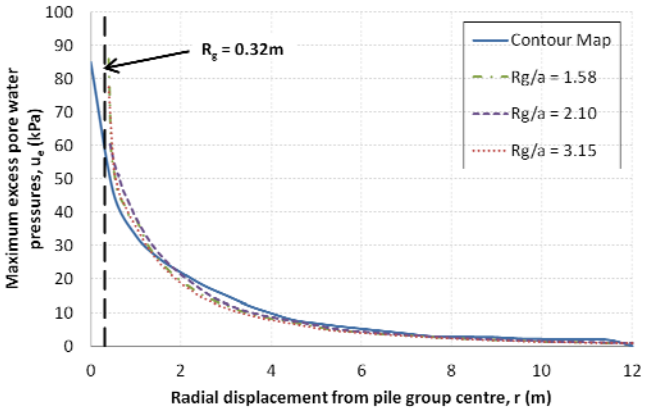

Figure 10a: Depth = 3m

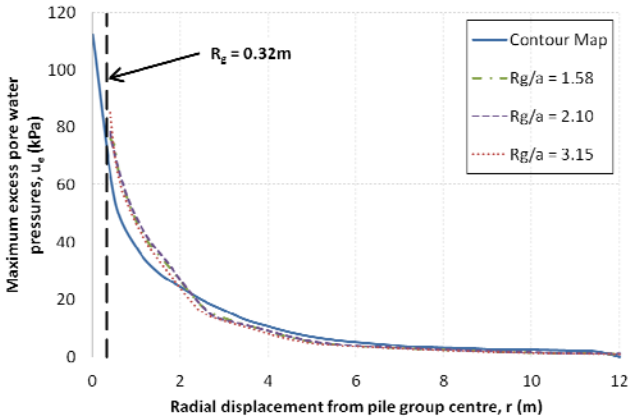

Figure 10b: Depth = 4m

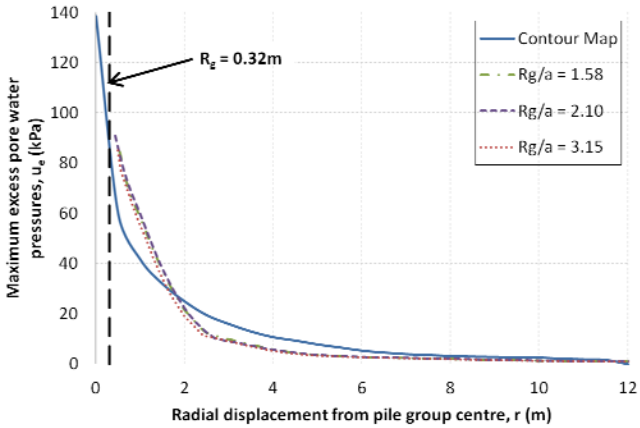

Figure 10c: Depth = 5m

Figure 11: Pore pressure dissipations for $c_h = 50m^2/year$

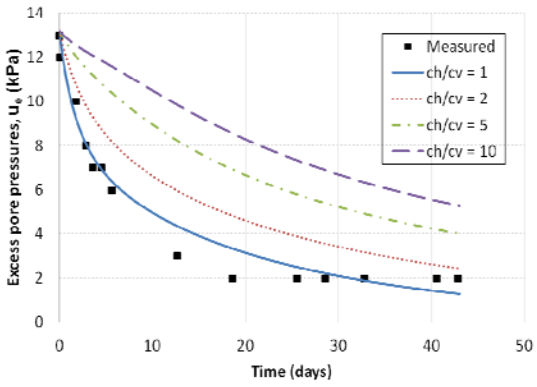

11a: Piezometer 2 (r = 3.3m, z = 2.85m)

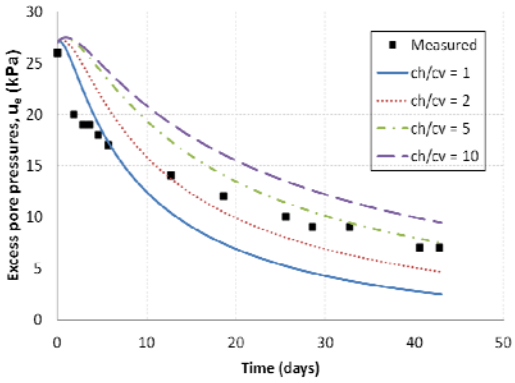

11b: Piezometer 4 (r = 1.6m, z = 3.35m)

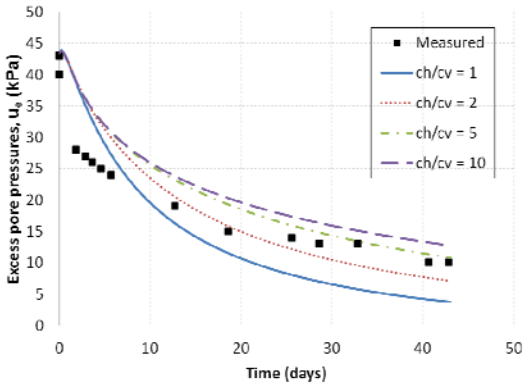

11c: Piezometer 6 (r = 0.75m, z = 3.9m)

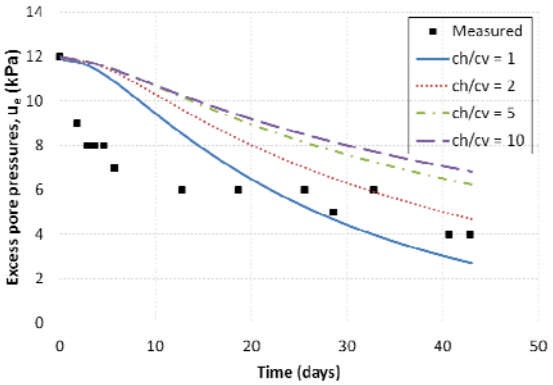

11d: Piezometer 5 (r = 2.35m, z = 7.4m)

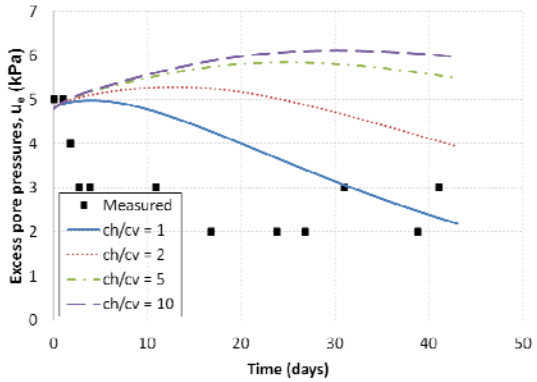

11e: Piezometer 1 (r = 6.3m, z = 5.4m)

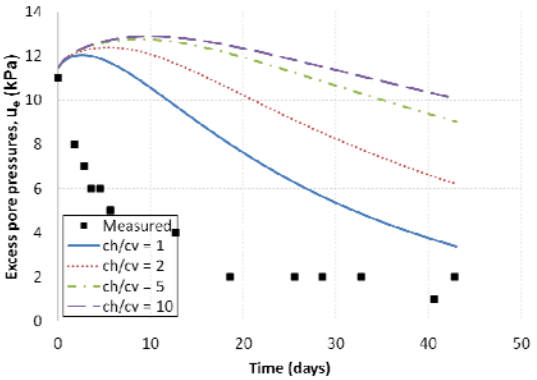

11f: Piezometer 7 (r = 3.75m, z = 4.7m)

Figure 12: Pore pressure dissipations for $c_h/c_v = 2$

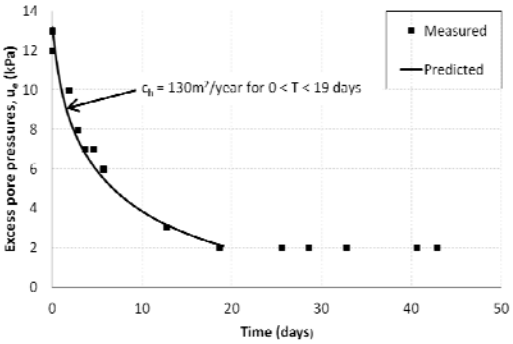

12a: Piezometer 2 (r = 3.3m, z = 2.85m)

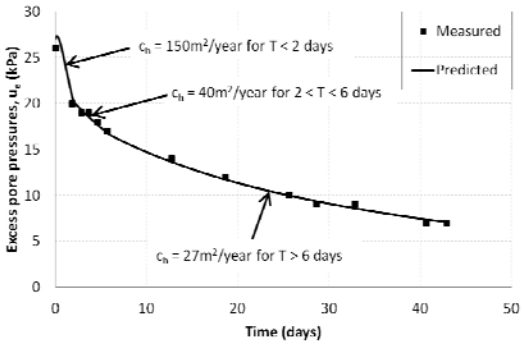

12b: Piezometer 4 (r = 1.6m, z = 3.35m)

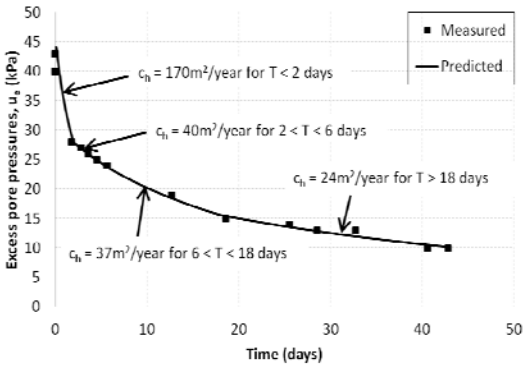

12c: Piezometer 6 (r = 0.75m, z = 3.9m)

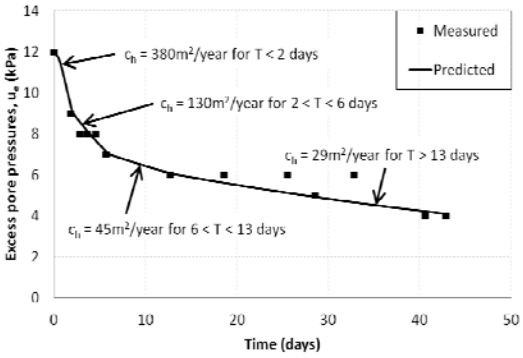

12d: Piezometer 5 (r = 2.35m, z = 7.4m)

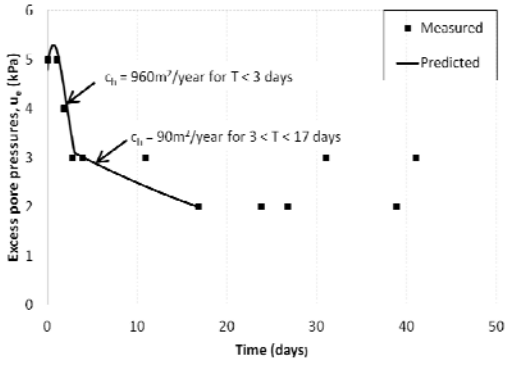

12e: Piezometer 1 (r = 6.3m, z = 5.4m)

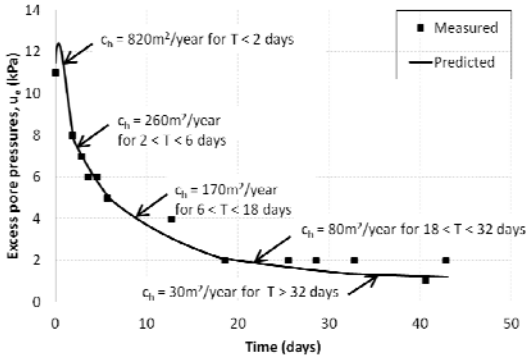

12f: Piezometer 7 (r = 3.75m, z = 4.7m)

Clay Fraction (%)	20 ± 10
Fines Content (%)	90 ± 5
Water Content (%)	60 ± 10
Plasticity Index (%)	35 ± 5
Organic Content (%)	11 ± 1
Peak Vane Strength (kPa)	22 ± 2
Over-Consolidation Ratio (OCR)	1.1 to 2.0
Friction Angle (^{o})	33 ± 1

Table 1: Typical properties of the Belfast *sleech*

Piezo. No.	Depth, z (m)	Radius from group centre, r (m)	u_0 (kPa)	$u_0 + u_e$ (kPa)	Comment
1	5.4	6.3	47	52	
2	2.85	3.3	21	34	
3	1.3	0.8	-	-	(refusal at shallow depth, no reliable data)
4	3.35	1.6	29	55	
5	7.4	2.35	71	83	
6	3.9	0.75	31	74	
7	4.7	3.75	39	50	
8	3.9	11.25	32	34	(increase very small)
9	2.5	20.85	13	n/a	(too distant to register pile group driving, but registered other adjacent activity)

Table 2: Details of pneumatic piezometer

	Fill	Silty Sand	Sleech	Sand
Depth (m)	0.0 - 1.0	1.0 - 1.7	1.7 - 9.0	9.0 - 12.0
γ_{unsat} (kN/m^3)	18.5	17.5	16.5	20
γ_{sat} (kN/m^3)	18.5	17.5	16.5	20
k_x (m/day)	1.000	2.592×10^{-5}	5.184×10^{-5}	8.64
k_y (m/day)	1.000	2.592×10^{-5}	2.592×10^{-5}	8.64
e_{init}	1.7	1.7	1.7	1.7
Φ' (^{o})	33	33	33	40
ψ (^{o})	0	0	0	0
c'$_{ref}$ (kPa)	0.5	0.5	0.5	0.5
m (power)	0.5	0.5	1.0	0.5
E_{oed}^{ref} (kPa)	25000	12000	9000	75000
E_{50}^{ref} (kPa)	25000	12000	9000	75000
E_{ur}^{ref} (kPa)	75000	48000	36000	225000
p_{ref} (kPa)	30	30	30	30
ν'_{ur}	0.25	0.25	0.25	0.25
OCR	-	2.0	1.2	2.0
POP (kPa)	15.0	-	-	-

Table 3: Soil parameters used in the Finite Element Model

γ_{unsat} = unsaturated unit weight, γ_{sat} = saturated unit weight

k_x = horizontal permeability, k_y = vertical permeability

e_{init} = initial void ratio, φ' = friction angle, ψ = angle of dilatancy, c'$_{ref}$ = cohesion

m = power (controlling stress-level stiffness dependence)

ν'_{ur} = unload-reload Poisson's ratio, OCR = Overconsolidation Ratio

POP = Pre-Overburden Pressure, p_{ref} = reference stress for stiffnesses

E_{oed}^{ref} = oedometric modulus, E_{50}^{ref} = secant modulus, E_{ur}^{ref} = unload-reload modulus